Article

Repurposing a two-component system-based biosensor for the killing of Vibrio cholerae

Premkumar Jayaraman, Maciej Bartosz Holowko, Jing Wui Yeoh, Sierin Lim, and Chueh Loo Poh

ACS Synth. Biol., **Just Accepted Manuscript** • Publication Date (Web): 25 Apr 2017

Repurposing a two-component system-based biosensor for the killing of *Vibrio cholerae*

Premkumar Jayaraman[2*], Maciej B. Holowko[1*], Jing Wui Yeoh[2], Sierin Lim[1] and Chueh Loo Poh[2]

[1]Department of Bioengineering, School of Chemical and Biomedical Engineering, Nanyang Technological University, Singapore
[2]Department of Biomedical Engineering, Faculty of Engineering, National University of Singapore, Singapore
[*]These authors contributed equally to this work.
Correspondence should be addressed to C.L.P. (biepcl@nus.edu.sg)

Abstract

New strategies to control cholera are urgently needed. This study develops an *in vitro* proof-of-concept sense-and-kill system in a wild-type *Escherichia coli* strain to target the causative pathogen *Vibrio cholerae* using a synthetic biology approach. Our engineered *E. coli* specifically detects *V. cholerae* via its quorum-sensing molecule CAI-1 and responds by expressing the lysis protein (YebF-Art-085), thereby self-lysing to release the killing protein (Art-085) to kill *V. cholerae*. For this report, we individually characterized the YebF-Art-085 and Art-085 expression and their activities when coupled to our previously developed *V. cholerae* biosensing circuit. We show that in the presence of *V. cholerae* supernatant, the final integrated sense-and-kill system in our engineered *E. coli* can inhibit the growth of *V. cholerae* cells effectively. This work represents the first step toward a novel probiotic treatment modality that could potentially prevent and treat cholera in the future.

Keywords: Cholera, biosensor, genetic circuit, sense and kill

Introduction

With the rapid emergence of synthetic biology, engineering complex genetic circuits into bacteria to address growing problems with infectious diseases and cancer is gaining increasing attention[1-2]. One pressing problem that remains a serious global threat is cholera, particularly in the developing world, where it claims thousands of lives each year[3]. Cholera, an infectious disease caused by the pathogen *Vibrio cholerae*, is most widely known for its massive epidemics and catastrophic consequences that have plagued humankind throughout history[4]. Part of the problem with cholera treatment strategies is the lack of an efficient therapy that would kill *V. cholerae* cells. The current state-of-the-art therapy is aimed at preventing death by alleviating the symptoms without killing the pathogen[5]. The currently available methods for *V. cholerae* infection prevention are also lacking[6]. Furthermore, the growing prevalence of antibiotic-resistant *V. cholerae* strains around the world is also alarming[7].

V. cholerae cells coordinate infection via an elaborate two-component-based quorum-sensing (QS) system[8-11]. Four proposed sensor proteins relay different signals from the environment via the phosphorelay protein LuxU to a shared response regulator called LuxO[12]. The sensor proteins responsible for processing signals coming from the environment in the form

of distinct chemicals are largely known to be membrane bound (e.g., CqsS and LuxPQ)[13-14]. CqsS detects CAI-1 (*S*-3-hydroxytridecan-4-one) as a QS signal that is highly specific to *V. cholerae*, whereas LuxPQ detects AI-2 as a QS signal that is present in many bacterial species[13]. Briefly, this QS system works as follows: When the density of *V. cholerae* cells in a given environment is low, the respective QS chemical concentrations are also low. These low levels make the sensor proteins act as kinases phosphorylating the key response regulator protein LuxO via the intermediate phosphotransfer protein LuxU. Next, the phosphorylated LuxO induces the expression of the regulatory sRNAs, which in turn control the expression of HapR, a master regulator protein responsible for switching 'ON' and 'OFF' the set of infection-related genes, such as cholera toxin (CT) and toxin co-regulated pilus (TCP)[15]. At high cell densities, the QS chemical accumulation in the environment is high. This accumulation results in the sensor proteins becoming dephosphatases, leading to the dephosphorylation and inactivation of LuxO, which causes the down-regulation of sRNAs and the cessation of virulence gene expression.

One possible therapeutic strategy to control cholera infection is to deploy synthetic gene circuits into commensal microorganisms to sense the presence of a pathogen and respond by expressing targeted or broad-spectrum antimicrobial agents[16-17]. We previously reported an *Escherichia coli* whole cell-based biosensor for *V. cholerae* detection[18]. This system was established by transferring the two-component CqsS QS system of *V. cholerae* into *E. coli.* This transfer resulted in our engineered *E. coli* becoming responsive to *V. cholerae* supernatant, which is known to contain CAI-1, the chemical detected by CqsS[19]. Our system also included a CRISPRi-based genetic inverter responsible for inverting and amplifying the signal coming from the *V. cholerae* phosphorylation cascade[20-21]. When no CAI-1 is present, the CRISPRi system prevents the expression of the signal protein GFP. However, when CAI-1 is present, CRISPRi activity is prevented, allowing the expression of GFP. In this study, we repurposed the sensor to be able to deliver an antimicrobial payload upon *V. cholerae* detection. In line with this approach, we adapted the "sense, lyse and release" therapeutic strategy based on our group's earlier work[16]. We faced two different key challenges to achieve this goal. First, we needed to identify a reliable antimicrobial protein to target *V. cholerae*. Concomitantly, the expression of the antimicrobial protein should have no impact on the growth of our *E. coli* host. Second, we had to identify an appropriate lysis protein to achieve host cell lysis to enable the rapid and effective release of the killing protein.

To address the first challenge, we focused our attention toward endolysins, which are enzymes produced by bacteriophages that digest both Gram-negative and Gram-positive cell walls[22]. One of the key examples of endolysin-based antibacterial proteins is the recent development of a novel class of antibacterials called artilysins[23]. Artilysin (Art-085) is the result of covalent fusion of the outer membrane-targeting peptide sheep myeloid 29-amino acid antimicrobial peptide (SMAP-29)[24] to the N-terminal of the KZ144 endolysin[25]. SMAP-29 can rapidly permeabilize Gram-negative bacteria's outer membrane and transport KZ144 through the outer membrane to degrade the peptidoglycan layer, thereby puncturing multidrug-resistant *Pseudomonas aeruginosa* and *Acinetobacter baumannii* strains in a rapid manner[25-26]. Because *V. cholerae* is also a Gram-negative pathogen, we tested the activity of Art-085 and report here for the first time that Art-085 exhibits strong bactericidal activity against *V. cholerae* strains.

Furthermore, the expression of Art-085 inside our *E. coli* host chassis did not affect its growth rate, making it an ideal killing molecule to express in sufficiently high quantities to target *V. cholerae* upon its release.

Next, to enable the effective and rapid release of Art-085, we tested the previously characterized Lysis E7 protein[16] to lyse our Art-085-expressing *E. coli* host chassis. We also characterized the expression of YebF (secretion tag protein)[27] fused to the N-terminus of Art-085. We hypothesized that upon reaching the periplasm through the YebF secretion pathway, Art-085 would presumably puncture and digest the outer membrane, thereby lysing the host cell. It has been proposed that YebF is secreted in a two-step process. In the first step, transportation of pre-YebF from the cytoplasm into the periplasm is achieved through the sec-dependent system in the inner membrane, where it is converted into mature YebF by leader peptidase I. Next, the mature YebF in the periplasm is transported into the medium by an unknown mechanism in the outer membrane[27]. As hypothesized, our results indicated that YebF-Art-085 as a lysis protein resulted in rapid and efficient lysis. Furthermore, the YebF-Art-085 fusion released into the medium during lysis had no antibacterial effect when tested against *E. coli* or *V. cholerae*. Thus, in the current work, we used the lysing property of YebF-Art-085 as a mechanism to release Art-085 killing protein. In the final stage, the sensor read out was replaced by the YebF-Art-085 gene, and we determined the optimum expression level of YebF-Art-085 that is required for effective lysis under the 'ON' state (CAI-1 present in the *V. cholerae* supernatant) and no lysis under the 'OFF' state (no CAI-1 in the *E. coli* supernatant).

Overall, we demonstrate how our final *V. cholerae* sense-and-kill genetic system in our engineered *E. coli* responds to the presence of *V. cholerae* supernatant by self-lysing (due to YebF-Art-085 lysis protein expression) and releasing Art-085 killing protein into the medium to kill *V. cholerae in vitro*. Our engineered *E. coli* effectively senses the presence of CAI-1 in the *V. cholerae* supernatant, resulting in the effective killing of *V. cholerae*. Although, our proof-of-concept genetic circuit to sense and target *V. cholerae* is in its infancy as a therapeutic option, we envision that this synthetic biology-based antibacterial strategy has exciting potential to prevent and treat cholera disease in the near future.

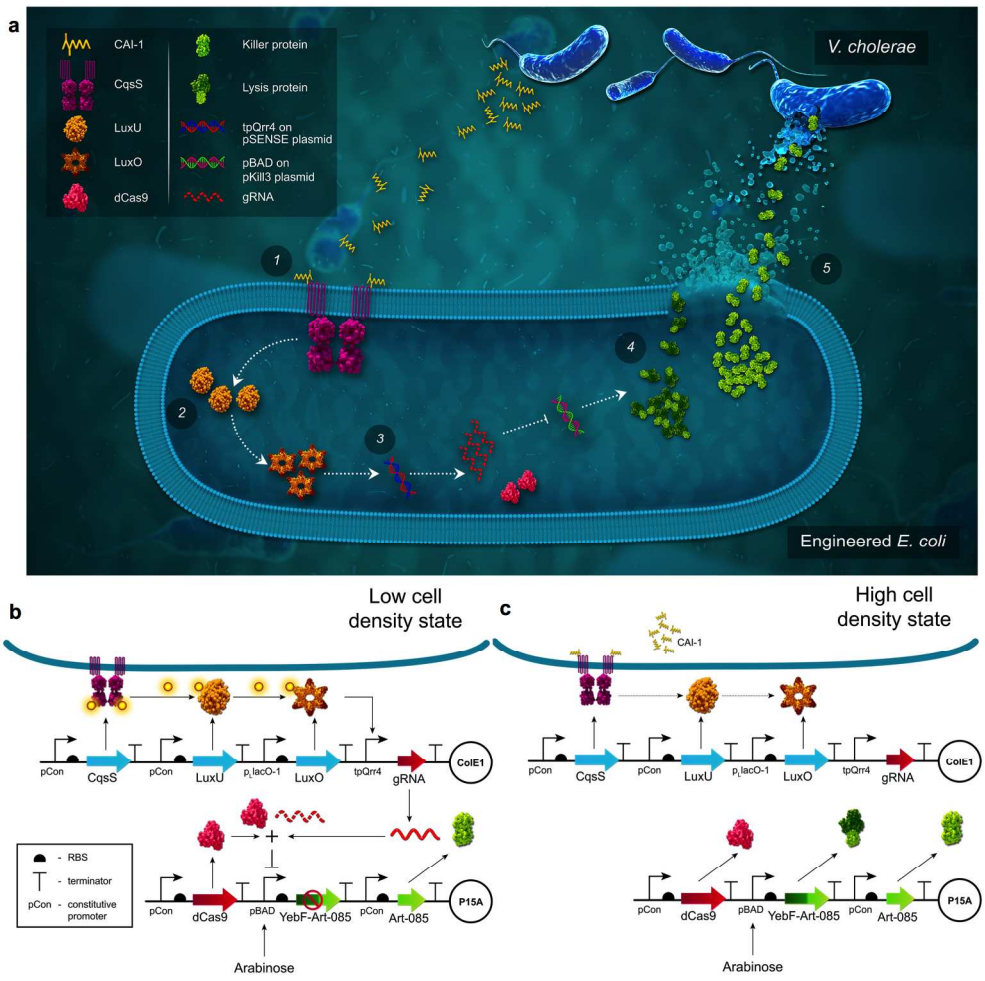

Figure 1. Design of our *V. cholerae* sense, lyse and kill system in *E. coli*. (a) General working principles of the designed circuit. 1) When the density of *V. cholerae* cells in the environment becomes sufficiently high, they produce the QS signalling molecule CAI-1 at high concentrations. Upon CAI-1 binding, the CqsS expressed in our *E. coli* is turned into a dephosphatase. 2) CqsS dephosphorylates LuxO via LuxU. 3) Dephosphorylated LuxO is unable to activate the transcription of gRNA at the tpqrr4 promoter in the pSENSE plasmid, thus stopping the repression of the lysis protein YebF-Art-085's promoter (pBAD in the pKill3 plasmid). 4) Thus, lysis proteins are produced in high quantities to rupture our *E. coli* host cell membrane. 5) Upon lysis, constitutively produced Art-085 killer proteins are released into the environment and subsequently kill the *V. cholerae* cells. (b) Genetic circuit design and working principles when there is no CAI-1 (low *V. cholerae* density). Autophosphorylated CqsS phosphorylates LuxO via LuxU, and phosphorylated LuxO activates transcription of gRNA by binding to the tpqrr4 promoter. Subsequently, the gRNA binds to the constitutively expressed dCas9, and the complex represses the expression of lysis protein YebF-Art-085. Thus, the constitutively produced Art-085 stays within the host cell and is not released due to the retained membrane integrity. (c) Genetic circuit design and working principles under high CAI-1 (high *V. cholerae* density) concentrations. The working principles are analogous to the explanations given in section (a) of this figure.

Results

The genetic architecture of our *V. cholerae* sensing and killing system is shown in Fig. 1. In the following sections, we present the results for the characterization of the killing and lysis proteins and how we layered them with our *V. cholerae* biosensor circuit into a final system that can target *V. cholerae* upon detection *in vitro*.

Killing and lysis protein characterization

As a first step, we sought to determine whether the expression of Art-085 affected the growth of our *E. coli* host strain. This information is important, as our host system is designed to constitutively express and release the killing protein through lysis upon detection of *V. cholerae*. Thus, the killing protein must be benign to the host cell until the cell is lysed. For this determination, a plasmid expressing Art-085 under the regulation of the arabinose-inducible pBAD promoter was constructed (pArt085) (Fig. 2a). Upon induction with 0.2% arabinose, our *E. coli* host chassis expressing the Art-085 gene experienced no noticeable growth reduction compared to control cells grown without arabinose induction (Fig. 2a). This result suggests that intracellular Art-085 expression does not impact the growth of our *E. coli* host, most likely because it cannot reach the peptidoglycan layer from the inside of the cell. Based on this result, we hypothesized that if a secretion protein (YebF) were tagged to Art-085, the resulting fusion protein could exert lysis activity on the host cell upon reaching the peptidoglycan layer and could be an effective lysis protein. To test this hypothesis, we fused the YebF gene to the N-terminal of Art-085 (YebF-Art-085), and we placed it under regulation of the pBAD promoter (pYArt085) (Fig. 2a). As expected, when induced with 0.2% arabinose, the expression of the YebF-Art-085 fusion protein resulted in significant lysis of the host cells, presumably caused by the YebF-Art-085 protein passing through the inner membrane and disrupting the peptidoglycan layer (Fig. 2a).

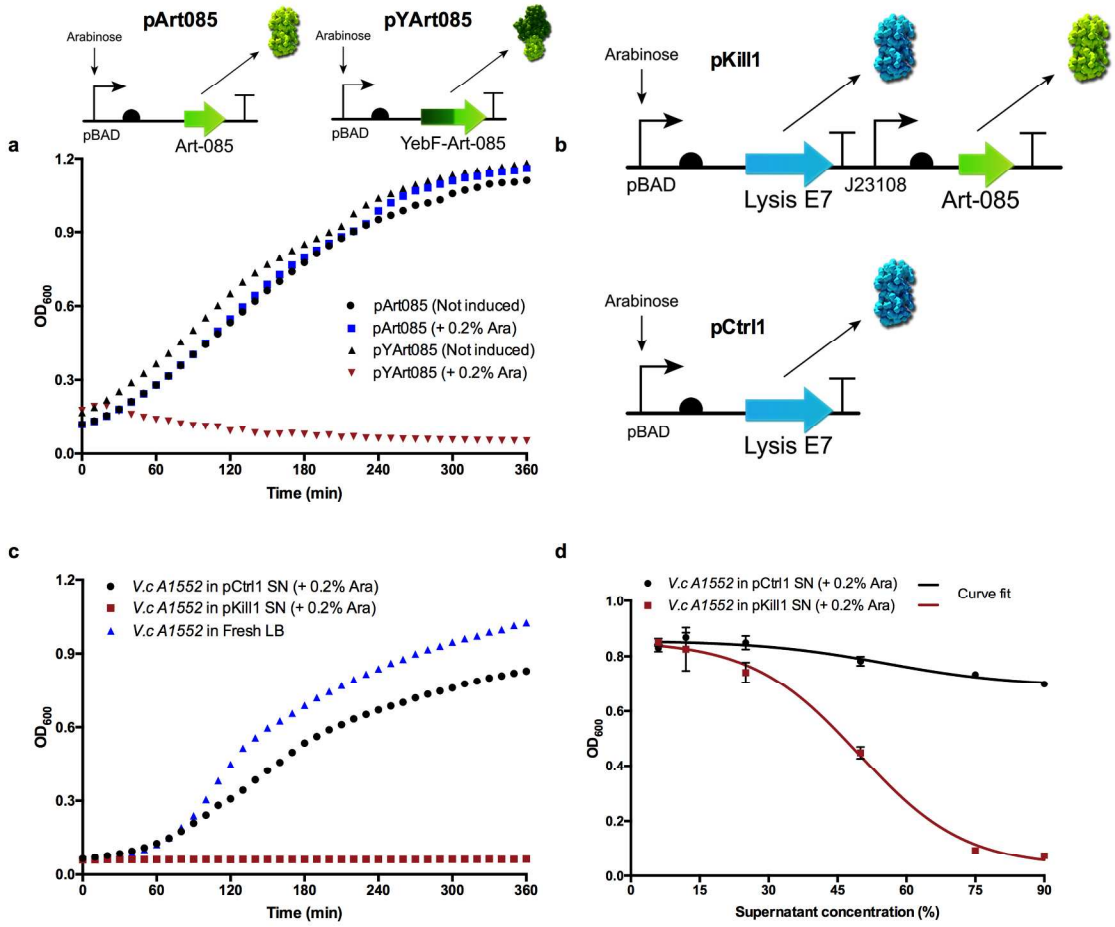

Figure 2. Characterization of Art-085 and YebF-Art-085 expression in *E. coli* and activity of Art-085 against *V. cholerae*. (a) Comparison of the growth curves of *E. coli* cells expressing either the Art-085 or YebF-Art-085 proteins. When *E. coli* cells transformed with pArt085 are induced with 0.2% arabinose, the growth of the *E. coli* cells is unchanged compared to that of the uninduced cells. This result indicates that Art-085 expression has no effect when expressed inside *E. coli* cells. In contrast, when cells transformed with pYArt085 are induced with 0.2% arabinose, they are lysed in a rapid manner compared with uninduced control cells. Genetic circuits are shown for the constructs used in this set of experiments. (b) Design of the circuits used to test Art-085 activity against *V. cholerae* cells. The upper circuit shows the construct (pKill1), in which Art-085 is constitutively expressed and released upon arabinose induction due to lysis E7 protein expression. The lower circuit shows the control construct (pCtrl1), which does not express Art-085 but still lyses upon arabinose induction. (c) Growth curve of *V. cholerae*-A1552 cells grown in the supernatant of *E. coli* cells carrying either the pKill1 or pCtrl1 plasmid induced with 0.2% arabinose. We also show *V. cholerae*-A1552 cells grown in fresh LB media for comparison. In the case of pKill1 supernatant induced with arabinose, the Art-085 proteins released upon lysis rapidly inhibit the growth of *V. cholerae*-A1552 cells upon exposure. In contrast, in the control supernatant (pCtrl1) induced with arabinose, the growth of *V. cholerae*-A1552 cells is slightly inhibited in comparison to cells grown with fresh LB. (d) Dose-response curves using the diluted supernatants of pKill1 and pCtrl1 cultures induced with arabinose. These data show that pKill1 supernatant retains its killing properties up to a 50% dilution. The best-fit curves for the dose-response data obtained are shown as solid lines. All data points represent the mean ± s.d. of three biological replicates.

Next, to examine the efficacy of Art-085 against the *V. cholerae* target strain, we constructed a pKill1 plasmid carrying the Art-085 gene and Lysis E7 gene (Fig. 2b). As a control, we also constructed a plasmid (pCtrl1) comprising only the Lysis E7 gene but lacking the Art-085 gene. Upon induction with 0.2% arabinose, host cells carrying the pKill1 plasmid lysed due

to Lysis E7 expression and released the killing protein Art-085 into the medium, whereas the control cell (carrying pCtrl1 plasmid) also lysed, but without the killing protein present. To confirm the inhibitory activity of Art-085, both killer and control supernatants were filter sterilized and exposed to the *V. cholerae* test strain, respectively, and OD_{600} was measured over time for 6 h. Cultures grown in the control supernatant lacking Art-085 showed normal growth while the cultures grown in the killing supernatant containing Art-085 showed high bactericidal activity against the *V. cholera*e test strain (Fig. 2c). We also performed dilutions of the collected supernatants to determine the dose-response curves. We find that ≥ 50% dilution of the killer supernatants inhibited the growth of *V. cholerae*, while the control supernatant has no detrimental effect on the growth (Fig. 2d and Supplementary Fig. 2a,b). Overall, this shows that Art-085 can be stably expressed inside the *E. coli* host chassis and is effective at inducing *V. cholerae* cell death.

Characterization of the system integrated with the sense, lyse and killing devices

After characterizing the reliability of YebF-Art-085 protein in lysing our *E. coli* host and the killing efficacy of Art-085 protein against *V. cholerae*, the next step was to integrate both the YebF-Art-085 and Art-085 genes into the existing *V. cholerae* sensor[18] to create the complete sense-and-kill system. The sensor is a two-plasmid based circuit, where the *V. cholerae* QS proteins control the expression of gRNA (first plasmid with a ColE1 origin) and gRNA coupled with dCas9 controls the expression of GFP (second plasmid with a p15A origin). The first step of the integration was to replace GFP with the YebF-Art-085 protein at the final point of the cascade of our previous sensor design. This replacement would allow lysis to be activated only with *V. cholerae* supernatant (CAI-1 present). One major difficulty that we faced in the replacement of constitutively expressed GFP in our sensor with YebF-Art-085 protein in the p15A origin plasmid was that the cells lysed during transformation. We were not able to generate the correct transformants on the plate, even with the co-transformation of the ColE1 origin plasmid expressing the gRNA to repress the constitutive promoter. Thus, we deduced that the constitutive promoter used to drive GFP in our sensor could be overly strong for YebF-Art-085 protein expression, meaning that the CRISPRi system could not prevent cell lysis due to insufficient repression of the promoter (BBa_J23115) driving the YebF-Art-085 expression. However, if we substituted a weaker promoter the expression level of the lysis protein might be overly weak, meaning that the cell would not lyse even upon *V. cholerae* detection. To circumvent this problem and to rapidly prototype the desired expression level, we modified the system so that the YebF-Art-085 protein would be expressed under the arabinose-inducible promoter pBAD. This change would also enable us to vary the expression level of YebF-Art-085 protein using arabinose to determine the optimal promoter strength. To accomplish this goal, the CRISPRi inverter's gRNA was redesigned to target pBAD instead of the previous constitutive promoter. After the new gRNA and pBAD were incorporated into the system, the GFP could be finally replaced with YebF-Art-085, resulting in the lysis-inducing plasmid pKill2. The final genetic circuit is shown in Fig. 1b ('OFF'-state) and 1c ('ON'-state), with the only difference being the lack of the Art-085 gene at this stage.

Fig. 3a shows the difference in OD_{600} after 4 h between our engineered *E. coli* cultures (co-transformed with pKill2 + pSENSE plasmids) grown in supernatants from cultures of two different bacteria: *E. coli*, non-activating (no CAI-1) as a control and *V. cholerae*, activating (CAI-1 present). The role of the supernatants here was to simulate the presence of the respective bacteria in our construct's growth environment. There was a visible inhibition of growth in cultures grown in *V. cholerae* supernatant compared with cells cultured in the *E. coli* supernatant at arabinose concentrations from 0 to 0.001% (Fig. 3a). However, there was no sign of lysis, which indicated that the pBAD was under-expressing the lysis protein. At an arabinose concentration of 0.005% (Fig. 3d), we achieved the desired effect – culture with *E. coli* supernatant showed slowed growth, but without evidence to suggest lysis, whereas culture with *V. cholerae* supernatant showed evidence of lysis. At concentration exceeding 0.005%, cultures grown in *V. cholerae* and *E. coli* supernatants both lysed, which suggests that pBAD was able to express the YebF-Art-085 protein beyond the CRISPRi system's ability to supress it. Nevertheless, this construct met the design criterion of having an arabinose concentration such that the activated construct (growing in *V. cholerae* supernatant) showed lysis but the control (*E. coli* supernatant) did not.

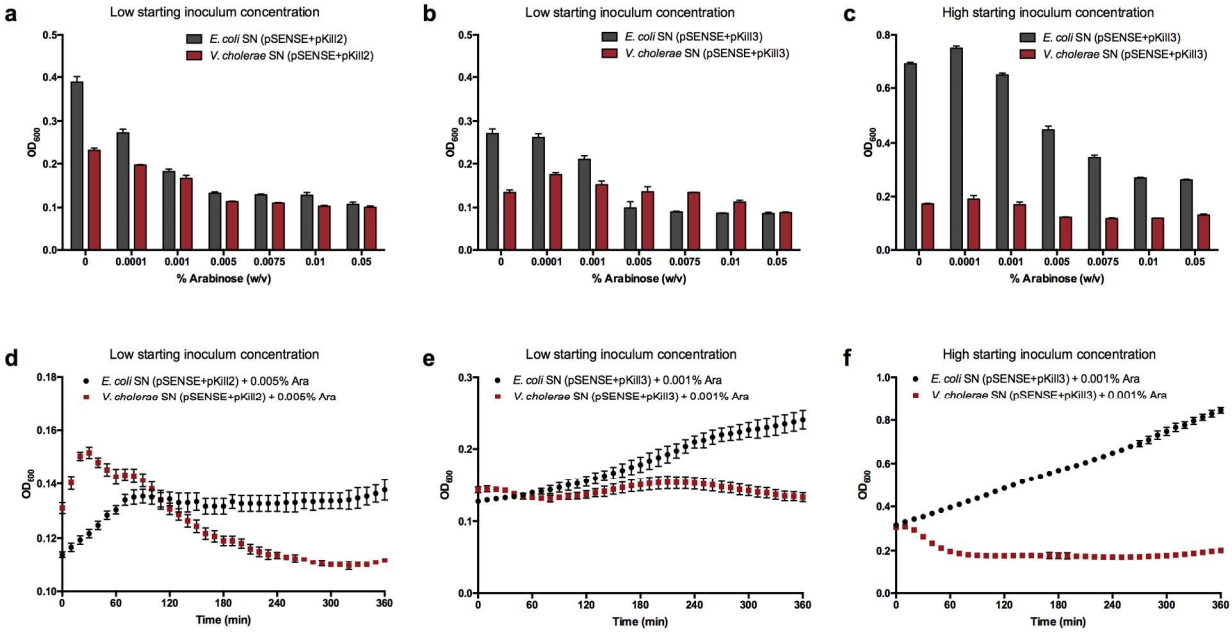

Figure 3. Characterization of the integrated sense, lyse and killing devices in our engineered *E. coli*. (a) Characterization of the sense-and-lyse device (pSENSE + pKill2 plasmids). The bar graph shows the differences in OD_{600} for *E. coli* cultures carrying the pKill2 plasmid grown in either *E. coli* or *V. cholerae* supernatant under increasing arabinose concentrations. (b, c) Characterization of the sense, lysis-and-killing device (pSENSE + pKill3 plasmids). (b) Low starting inoculum concentration. (c) High starting inoculum concentration. Data were collected 4 h after induction with different arabinose concentrations. (d). Growth curve of *E. coli* transformed with the pSENSE + pKill2 plasmids after induction with 0.005% of arabinose. (e, f) Growth curve of *E. coli* transformed with the pSENSE + pKill3 plasmids after induction with 0.001% of arabinose. (e) Low starting inoculum concentration. (f) High starting inoculum concentration. These data show that *E. coli* cultures carrying either the pKill2 or pKill3 plasmid grow normally when grown in *E. coli* supernatant (no CAI-1, 'off' state). In contrast, the cultures grown in *V. cholerae* supernatant (CAI-1 present,

'on' state) undergo lysis shortly after the start of the culture, thereby releasing the killing proteins. All data points represent the mean ± s.d. of three biological replicates.

To test this circuit, we added Art-085 killing protein expression into the previous pKill2 plasmid and created the pKill3 plasmid. Because we already demonstrated that Art-085 can be safely expressed in *E. coli* under a constitutive promoter, we decided to express it in this construct using an even stronger constitutive promoter with a strong RBS to ensure that a high concentration of Art-085 would be produced and subsequently released upon cell lysis. Fig. 1b, c show the full design of the system and how it behaved with and without CAI-1 in the extracellular environment.

Fig. 3b shows the OD_{600} difference after 4 h between our engineered *E. coli* cultures (co-transformed with pKill3 + pSENSE plasmids) grown in both *E. coli* (control) and *V. cholerae* (activating) supernatants. The system showed signs of lysis in a similar manner as the system without Art-085 incorporated; however, there were some significant differences. First, the general final OD_{600} of the cultures was lower than that of the lysis-only cultures (when the killer protein expression was not present). Second, the desired characteristic of the culture was achieved at a lower arabinose concentration, namely, 0.001% (Fig. 3e). Both effects could be due to the lysing of cells releasing high amounts of killing protein (Art-085) into the extracellular environment, which then accelerated the lysis rates of other cells by acting from outside the cells (positive feedback mechanism). To test this hypothesis, we repeated the cultures but with a less dilute inoculum (see the Materials and Methods section). Taking this approach, we achieved a higher starting inoculum at the point of the addition of arabinose. If our hypothesis is correct, then with a higher OD_{600} at the point of the addition of arabinose, more Art-085 should be released due to the lysing of cells, and this positive feedback effect should be even more profound. The behaviour of such cultures with different arabinose concentrations is shown in Fig. 3c. The striking difference was that the constructs became more sensitive to *V. cholerae* supernatant under such conditions, where the culture showed obvious signs of lysis even without the addition of arabinose. The characteristics of the system were vastly improved with the addition of 0.001% arabinose, with cultures in *E. coli* supernatant growing to a high OD_{600} and the cultures in *V. cholerae* supernatant exhibiting fast lysis (Fig. 3f). This result reinforces the view that Art-085 improves the lysing capabilities and that the observed effects are due to the combined action of the lysis-and-killing proteins.

In silico mechanistic approach to study the positive feedback mechanism

To gain further insights into the hypothesis of the existence of a positive feedback mechanism whereby killing proteins (Art-085) released from the lysed cells further accelerate the lysis rates of other cells, an *in silico* modelling approach was employed to characterize the details of the process in a quantitative manner. A kinetics model based on ordinary differential equations (ODEs) was developed to elaborate the dynamics of the system components, including the constitutively generated intracellular killing proteins (Art-085), the extracellular killing proteins, and the cell density, represented by OD_{600}. Data from *E. coli* (control) and *V. cholerae* (activating) supernatants were included in the simulations for comparison purposes. As shown by the experimental data (Fig. 3e, f), the fold difference between cultures with *E. coli* and *V.*

cholerae supernatants, respectively, grown at a higher starting OD_{600} were significant greater than those of cultures grown at a lower starting OD_{600}. This profound distinction between a high and low starting OD_{600} suggests the potential influence of a positive feedback mechanism induced by a high concentration of extracellular killing proteins in the growing medium. These data were used to facilitate the modelling effort.

The model was developed in four steps. First, the constitutive transcription and translation of killing proteins (Art-085) were characterized and constructed based on the experimental data. Second, the lysis-and-killing mechanisms were modelled. Next, the cell density (OD_{600}) model was incorporated to reproduce the observed experimental data, as shown in Fig. 3e, f. Finally, the model was used to provide insights into conditions under varying parameter values that would be difficult if not impossible to obtain experimentally. Because experimental data have indicated that 0.001% arabinose is the optimal concentration to induce the activated construct (under *V. cholerae* supernatant) to lyse cells as opposed to the control (*E. coli* supernatant), observations under 0.001% arabinose were considered for the entire development of the model.

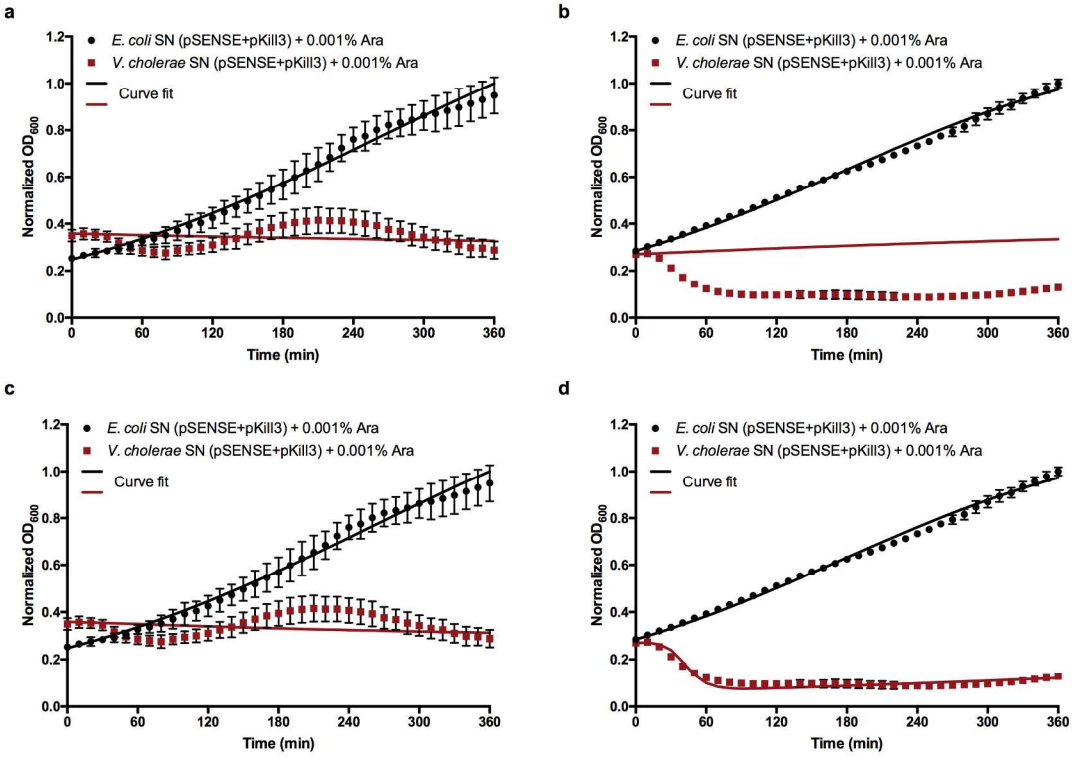

Figure 4. *In silico* mechanistic approach to study the positive feedback mechanism induced by the extracellular killing protein Art-085. (a) Simulated normalized OD_{600} for cultures growing under *E. coli* supernatant (control) and *V. cholerae* supernatant (activated) conditions at a low starting OD_{600} without considering the positive feedback killing effect. It was presumed that there was a small proportion of cells lysed when induced by 0.001% arabinose in culture with *V. cholerae* supernatant due to the presence of CAI-1, whereas the engineered *E. coli* grown in *E. coli* supernatant underwent normal growth, and no lysis occurred. (b) Simulated normalized OD_{600} for cultures growing at a higher starting OD_{600} without the positive feedback mechanism. The model could not reproduce the experimental observation using the same lysis proportion for the culture grown with *V. cholerae* supernatant due to the larger fold difference between

cultures under the control and activated conditions. (c) Simulations after incorporating the positive feedback killing mechanism for cultures growing under a low starting OD_{600}. (d) Simulations for cultures with a high starting OD_{600} after considering the secondary positive feedback effect. The model shows good agreement with the experimental data for both cultures with different supernatants.

To test the hypothesis of the positive feedback mechanism, we first simulated the conditions without secondary killing (positive feedback effect) for both cultures growing at a low and high starting OD_{600}. Fig. 4a, b show the corresponding simulations, respectively. In all cases, it was assumed that there was no lysis in the control samples (*E. coli* supernatant) at 0.001% arabinose induction due to suppression by the CRISPRi system as opposed to lysis induced in the activated construct grown in *V. cholerae* supernatant in response to the presence of CAI-1. The engineered *E. coli* cultures exhibited a normal growth pattern in both control studies, whereas a significant reduction in OD_{600} was emulated under both starting OD_{600} levels in *V. cholerae* supernatants. However, there was a lack of fit for the cultures starting with a high OD_{600} under *V. cholerae* supernatant compared to a low starting OD_{600} when the same parameter values were applied for both conditions. We then incorporated the secondary killing model and evaluated the fitting of both sets of data, as shown in Fig. 4c, d. With the positive feedback mechanism, the model showed a good fit for the experimental data for the culture with a high starting OD_{600}, which corroborates the notion that Art-085 killing proteins released due to lytic activity could exert a secondary killing effect on other cells from the outside, consequently accelerating the reduction in the OD_{600}. This process would constitute a positive feedback mechanism. (A complete description of the model and additional model validations are provided in the Supplementary Material).

After developing the model, we proceeded to gain more insights into the effects of the parameters on the system's behaviour. Based on our simulations, two key aspects of the model were considered to obtain a reasonably good fit for the experimental data for the culture growing with a high starting OD_{600}: the positive feedback killing effect and the degradation of the extracellular killing proteins. The extent of the positive feedback determined the rate of decrease (slope) in the OD_{600}, whereas the extracellular degradation rate of the killing proteins governed the steady-state level. To this end, we examined how the system behaves under different killing rates and degradation rates by plotting both 2-D and 3-D contour plots (Fig. 5a-d) of two output quantities (the gradient of the OD_{600} and the steady-state level, respectively) over increasing killing and degradation rates. Based on the formalism we used, we intuitively hypothesized that an increase in the killing rate would increase the negative slope of the OD, whereas an increase in the degradation rate would increase the ultimate steady-state OD_{600} value due to a reduction in the extracellular concentration of killing proteins. As shown by the contour plots, the highest negative gradient in conjunction with the lowest OD_{600} indicates that the highest killing efficiency occurs at the highest killing rate and lowest degradation rate. In the case without considering the degradation of extracellular killing proteins ($D_{deg} = 0$), the killing rate must be extremely low ($V_{kill} < 0.1$ min^{-1}) to reach the steady state observed in the experiment when a high starting OD_{600} is used (Fig. 3f), whereas a killing rate higher than 0.1 min^{-1} would reach the lowest OD_{600} observed wherein all cells were killed. However, a recent study showed the rapid killing efficiency of Art-175, a homologue of Art-085, in which the entire mode of action, from puncture of the cell wall to increased bulging of the cytoplasmic membrane to abrupt cell lysis,

took approximately 4.4 min after adding Art-175, which is equivalent to a killing rate of 0.227 min^{-1} [25]. At such a high killing rate, our model has predicted a 0.05 min^{-1} degradation rate (an approximate half-life of 13.9 min) for the extracellular killing proteins to reproduce the steady state reached as reported in the experimental observation with the high starting OD_{600}. This modelling work provided a means to study a hypothesis derived based on experimental data that would otherwise be difficult to prove experimentally. Our model suggests the potential existence of a positive feedback killing effect induced by a high concentration of extracellular killing proteins, and the degradation of extracellular killing proteins. To improve the system killing efficiency, the model also implies that a more stable killing protein with low degradation rate and a killing rate of more than 0.1 min^{-1} could be used to effectively kill the cells and reach the lowest OD_{600}. As can be observed from Fig. 5a, a notable wide range of killing rates and degradation rates, as signified by deep blue area, could be used to achieve this full killing purpose. The highest efficiency could come from a killing peptide with a killing rate of more than 0.95 min^{-1} and a degradation rate of less than 0.01 min^{-1} (Fig. 5c).

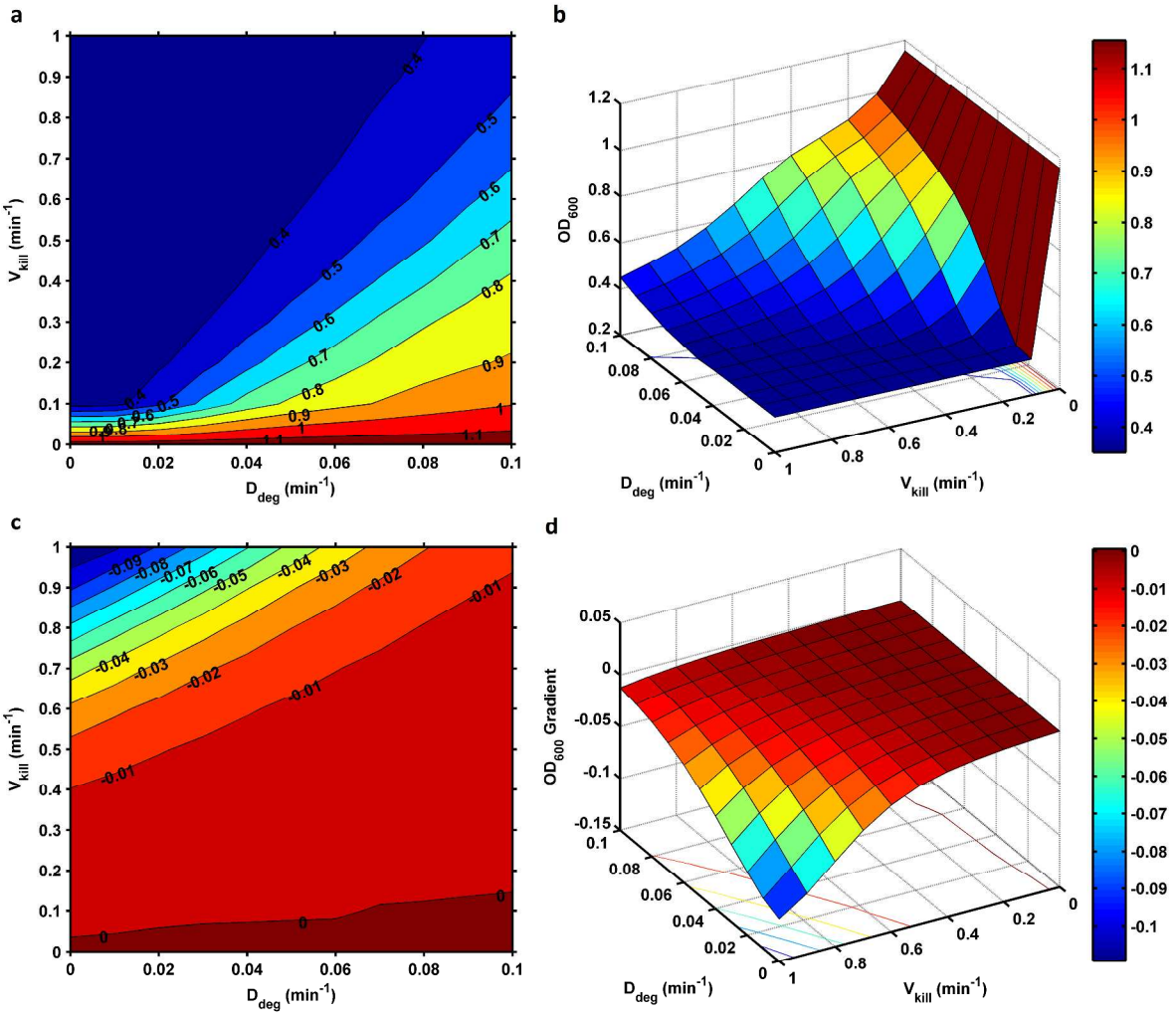

Figure 5. Model analysis to investigate the influence of varying two key parameters' values (D_{deg} and V_{kill}) on the model's outputs. (a) 2-D contour plot displaying the isolines of different OD_{600} steady-state values after

300 min under varying D_{deg} (x-axis) and V_{kill} (y-axis) conditions. The constant colours filled between the isolines correspond to the different values specified in the colour map. (b) Representative 3-D contour plot from (a) with the OD_{600} output displayed on the z-axis. (c) A 2-D contour plot showing the different OD_{600} gradients estimated from 12 to 14 min from the OD time-series plot. (d) Representative 3-D contour plot from (c) with the OD_{600} gradients presented on the z-axis.

Our system delivers a killing payload upon detection of *V. cholerae*

With the full system constructed and characterized, we next tested its killing capabilities against *V. cholerae*. The killing was tested with undiluted supernatants using our engineered *E. coli* cultures (carrying pSENSE + pKill3 plasmids) that were cultured separately in *E. coli* and *V. cholerae* supernatants and later induced with 0.001% arabinose. The supernatants were later inoculated with *V. cholerae* cells and moved to microplate for characterization (Fig. 6a). The cultures with *E. coli*-induced supernatant exhibited a similar growth rate as *V. cholerae* growing in fresh LB. In contrast, the cultures with the *V. cholerae*-induced supernatant were unable to grow, and the rapid killing of the cells was similar to the results obtained in our previous tests (Fig. 2c). To determine whether this result was simply an effect of the supernatant itself (depletion of nutrients), we also performed a similar test with a construct that does not express Art-085 (Fig. 2b). In this test, only *V. cholerae* supernatant was used, and the engineered *E. coli* cultures (carrying pSENSE + pKill2 plasmids) were induced with a high arabinose concentration (0.05%) to ensure complete lysis of the cells to simulate what occurs in our lysis-killing construct (where full lysis is achieved at lower arabinose concentrations than in the lysis-only construct) (Fig. 6b). The results showed that even supernatant from fully lysed, lysis-only cells was unable to impact *V. cholerae* growth in any significant way, which reinforced the interpretation that the killing is due to the assumed (because of a strong promoter and the use of RBS for expression) high concentration of Art-085 released.

To ensure that the *V. cholerae* cells were dead and not merely inhibited, we performed a time-kill assay in which we plated the *V. cholerae* cultures exposed to the supernatants of our engineered *E. coli* carrying the final system grown in *E. coli* (control) or *V. cholerae* (activating) supernatant induced with 0.001% arabinose on agar plates at different time points. The results in Fig. 6c,d show the change in the CFUs of cultures grown in *E. coli*-induced supernatant and *V. cholerae*-induced supernatant. Cultures grown in *E. coli*-induced supernatant exhibited the expected steady growth in CFUs over time. In contrast, *V. cholerae*-induced supernatant cultures exhibited a drastic reduction in CFUs starting at 30 min, with plates at the 60 min mark showing no viable colony growth. This result concurs with results achieved for other bacteria tested against Art-085[25]. In addition, from our colony counting experiments we can estimate that the OD_{600} of 2 equals around 10^9 CFU of *V. cholerae*. This was the density at which our overnight *V. cholerae* supernatants was obtained. The results show that our *E. coli* system was activated at a CAI-1 concentration characteristic of this density of *V. cholerae.* We estimated that the threshold would be about half of this amount of CFUs. This estimation is based on our earlier work in which a ratio of 1:1 of supernatant to fresh LB generated visible difference in GFP fluorescence/OD_{600} between cultures in *V. cholerae* and *E. coli* supernatant whereas ratios of 5:95 and 30:70 did not show at least 50% difference which we set as a satisfactory threshold value for sensor activations[28]. The colony counting comparison results show that our *E. coli* in

density of 10^8 CFU[29] (OD of 0.1-0.2 as per Fig. 3c) is able to produce enough killing protein to kill *V. cholerae* in density of 10^8 CFU very effectively. We performed an agar overlay assay to further visualize the inhibitory effects of our engineered *E. coli* on *V. cholerae*. The plate was divided into four parts, and three drops of supernatant from the engineered *E. coli* grown in either *V. cholerae* or *E. coli* supernatants and induced with 0.001% arabinose were added to each quadrant before overlaying with soft agar mixed with *V. cholerae* cells (Fig. 6e). After 4 h of incubation, there were evident plaques visible in the parts of the plate where the supernatant of the engineered *E. coli* induced with *V. cholerae*-induced supernatant drops was added. However, after 6 h, the plaques were no longer visible, possibly indicating limited thermal stability for Art-085 from the supernatant. Overall, our results suggest that our engineered *E. coli* carrying the final system, which includes CAI-1 sensing, YebF-Art-085-based lysing and Art-085-based killing devices, can effectively inhibit the growth of *V. cholerae in vitro*.

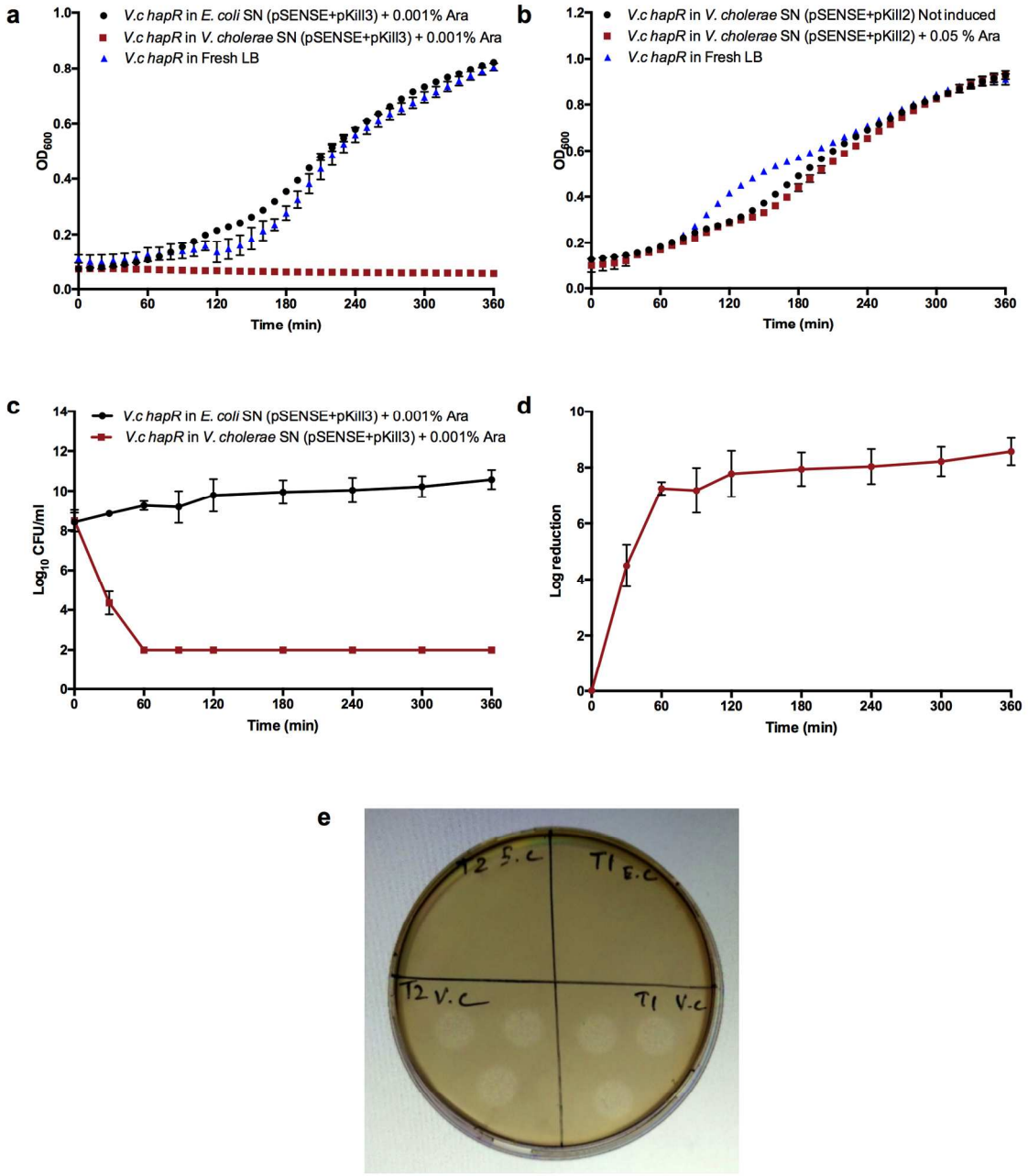

Figure 6. Characterization of *V. cholerae* growth with our sense-and-kill system. (a) Growth curve of *V. cholerae* cultures exposed to the supernatant of *E. coli* cells carrying the pSENSE + pKill3 plasmids grown in either *E. coli* or *V. cholerae* supernatants induced with 0.001% arabinose. We also show *V. cholerae* cells grown in fresh LB media for comparison. The growth of *V. cholerae* cells in fresh LB and in *E. coli* supernatant-induced cultures (carrying the pSENSE + pKill3 plasmids) progresses similarly, whereas the *V. cholerae* supernatant-induced cultures (carrying the pSENSE + pKill3 plasmids) show rapid inhibition of *V. cholerae* growth. This result suggests that our engineered *E. coli* with its sense, lyse-and-kill genetic circuit can detect CAI-1 in the *V. cholerae* supernatant and responds by lysing the *E. coli* cells (by expressing YebF-Art-085) to release the killing protein Art-085 into the media. The released Art-085 in the supernatant rapidly inhibits the growth of *V. cholerae* cells. (b) Growth curve of *V. cholerae* cultures exposed to the supernatant of *E. coli* cells carrying the pSENSE + pKill2 plasmids that were previously grown in *V. cholerae* supernatant induced with 0.05% arabinose or uninduced. We also show the growth of *V. cholerae* cells in fresh LB media for comparison. These data show no significant differences in growth rate for *V. cholerae* cells with only the

sense and lysis devices in the circuit. (c) Time-kill curve analysis of *V. cholerae* cells grown in the supernatant of *E. coli* cells carrying the pSENSE + pKill3 plasmids that were previously exposed to *E. coli* or *V. cholerae* supernatants induced with 0.001% arabinose. Cell viability was measured by CFU count after 14 h. Beyond the 60 min mark, all *V. cholerae* cultures grown in the *V. cholerae*-induced supernatant show CFU levels below 100 CFU, the lower limit of detection for this method. (d) Log reduction in CFUs for the same cultures as in (c). (e) Agar overlay assay of *V. cholerae* cells after exposure to *E. coli* and *V. cholerae*-induced supernatant of *E. coli* cells carrying the pSENSE + pKill3 plasmids. The photograph shows the plate after 4 h of incubation. The labels are T1 and T2 for tests 1 and 2 (two biological replicates), respectively, and Ec (*E. coli*) and Vc *(V. cholerae*) indicate the supernatants. *V. cholerae* cells exposed to the supernatant of *E. coli* carrying the pSENSE + pKill3 plasmids grown in *V. cholerae* supernatant displayed clear inhibition zones. This result suggests that the system produces sufficient Art-085 to exhibit bactericidal activity. All data points represent the mean ± s.d. of three biological replicates.

Discussion

In this work, we have constructed and characterized the first genetic circuit in *E. coli* that is capable of sensing *V. cholerae* and responding with self-lysing to release killing proteins that target *V. cholerae*. We achieved this system by modifying our previously reported *V. cholerae* sensor[18] and layering it with a lyse-and-kill circuit for *V. cholerae* (Fig. 1a). The mechanism of action is as follows: When a *V. cholerae*-specific QS signal (CAI-1) is present, our *E. coli* engineered with a QS phosphorylation cascade detects CAI-1, resulting in the sensor proteins becoming dephosphatases and thus inactivating LuxO. Inactivated LuxO is unable to bind to the pQrr4 promoter, leading to the down-regulation of gRNAs. Thus, CRISPRi activity is repressed, leading to the expression of YebF-Art-085 protein, which induces lysis of the host cell and thereby releases the accumulated Art-085 (which is constitutively expressed) (Fig. 1c). In contrast, when CAI-1 is absent, the phosphorylation cascade proteins engineered into our *E. coli* act as kinases, and phosphorylated LuxO binds to pQrr4, up-regulating gRNA synthesis. The activated CRISPRi complex represses YebF-Art-085 expression, resulting in no lytic activity and thereby preventing the release of Art-085 (Fig. 1b).

We followed a systematic approach to build this complex genetic circuit[30]. First, we showed that Art-085 can be expressed directly in the host cell without impacting its growth, which makes its suitable for bacterial delivery systems such as the one presented in this work (Fig. 2a). Second, we characterized the killing potential of Art-085 against *V. cholerae*, and we are the first to report that Art-085 rapidly inhibits *V. cholerae* growth (Fig. 2b). According to the presented results, Art-085 is able to kill *V. cholerae* cells to levels lower than 100 CFU/ml within 1 h, which is comparable to other known antibiotics, but possibly without the effect of resistance acquisition over time[25]. This finding adds another bacteria species to the extensive list of organisms susceptible to Art-085, which emphasizes its wide efficacy[25-26, 31]. However, two possible drawbacks of Art-085 must be underlined. The fact that *V. cholerae* was able to overgrow the plaques visible on our agar plate assay after 6 h could presumably indicate that Art-085 has limited heat stability. Its broad efficacy can also be seen as a drawback – such treatments could affect the commensal microbiome of humans, which is highly undesirable. Third, we characterized the fusion of the YebF secretion protein to the N-terminal of Art-085, and we report here for the first time that the fusion protein (YebF-Art-085) induces a rapid lysing activity in our *E. coli* host cell (Fig. 2a). This capability may make YebF-Art-085 an ideal lysis

molecule, as it rapidly induces lysis and can be used as a modular component to assemble novel synthetic circuits.

Once we had characterized the individual killing and lysis devices, the next step was to integrate them into our previous sensor circuit. Our group's sensor system was designed to be modular. The intent was to be able to replace the GFP reporter with other modules, such as the lysis-and-killing modules developed in this paper. The key challenge was that different genetic parts often require different expression levels to be effective. Because of the incorporation of a CRISPRi inverter, it was easier for the system to be redesigned for the expression of other proteins as the final endpoints of the circuit requiring different expression levels. With CRISPRi, one can simply find (or design) a suitable gRNA-promoter pair for the task. The short length of the parts to be changed (tens of base pairs) for this pair replacement is also a considerable advantage when DNA manipulation is considered. In the case of this study, we achieved our goal by replacing the constitutively expressing signal protein (GFP) from our previous sensor with the arabinose-inducible pBAD promoter to drive lysis protein production. For this approach to work, we modified our previous sensor to express anti-pBAD gRNA under the pQrr4 promoter. Coupling CRISPRi with the inducible pBAD promoter enabled us to achieve rapid prototyping of the system (Fig. 3). The alternative, creating a library of different constitutive promoters to find one that would express the lysis protein at a sufficiently high level to lyse the cell and be readily repressed by the dCas9 complex at the same time, would be labour intensive and time consuming. By taking this approach of using an inducible promoter, we were able to test different expression levels at the same time, which shortened our testing time considerably. Now that the appropriate expression level has been found, the search for a suitable constitutive promoter (of comparable expression and repression levels) can be initiated to avoid the need to add arabinose in the future. In addition, our *in silico* model helped us better understand the behaviour of our system after the addition of Art-085 (Figs. 4 and 5), reinforcing the utility of computer models in biological design.

This study is not the first time that commensal *E. coli* has been engineered as a potential therapeutic option for *V. cholerae*. Previously, Focareta et al. engineered an *E. coli* strain to express GM_1 ganglioside on its surface to adsorb the cholera toxin (CT), thereby reducing *V. cholerae* virulence[32]. Recently, Duan and March[33] engineered a probiotic *E. coli* to secrete CAI-1 to achieve a quorum quenching effect, and pre-treatment with this strain has been shown to greatly increase survival in infant mice to over 90% following ingestion of *V. cholerae*. However, both of these therapeutic strategies are limited by the possibility that the recombinant receptor mimic or the expression of autoinducer CAI-1 might elicit an immunological response in the host system[32-33]. Additionally, neither of these strategies addresses *V. cholerae* eradication, which is the root cause of pathogenesis. In this paper, our system is designed to self-lyse to kill *V. cholerae* cells upon detection, which has the added advantage of potentially stopping the spread of the infection. To the best of our knowledge, this is the first time a synthetic *V. cholerae* sense-and-kill gene circuit has been developed for commensal *E. coli*. The genetic circuit presented in this work may be seen as the first stage of a process aimed at developing a new therapeutic option for *V. cholerae*. This goal could be achieved by modifying the host bacterium such that it can survive in the human gastrointestinal (GI) system, where *V. cholerae* is known to invade.

The modified bacteria with the killer system could potentially be activated in the GI tract by the presence of *V. cholerae* and kill it. The infective dose for *V. cholerae* is estimated to be around 10^6 organisms[34] and our system was shown to kill concentrations higher than this (Fig. 6c) which would reinforce its potential use. Future research, including studying the *in vivo* efficacy of our engineered *E. coli* in direct disease-relevant animal models, is necessary to elucidate its effect as a combined prophylactic and therapeutic against cholera. The system could be optimized further, by tuning some parts of it to improve sensitivity and/or efficacy. For example, CqsS could be mutated at its active site to make it more sensitive to CAI-1 so it would activate the cascade at lower CAI-1 concentrations. Promoters for the lysis and killing proteins could also be tuned so that they would express more of their respective proteins to make the lysis and killing more effective. In addition, our model suggests that having a killing protein with lower degradation rate and increased killing rate would further improve the killing efficiency of the system. Nevertheless, our tests show that the concept is viable, and with further development, this approach could be used to potentially prevent and treat cholera in the near future.

Materials and Methods

Strains, DNA sequences and plasmids

All transformations were performed using TOP10 (Invitrogen; Carlsbad, CA, USA) or Beta10 (New England Biolabs; Ipswich, Massachusetts, USA) *E. coli* strains, and the cells were used after a maximum of two passages from the commercial tube supplied by the vendor. All microplate experiments were performed in the MG1655 (K-12) *E. coli* strain unless otherwise stated. The *V. cholerae* strains used in the study include the following: the Vc-A1552-Tn7 smooth strain tagged with GFP and gentamicin (Gm^R) resistance[35], which natively produces CAI-1, was used to generate the activating supernatant and for the initial characterization of the Art-085 antibacterial activity; and Vc-*hapR* RFP (*ΔhapR*, mTn10-DsRedExpress, Amp^R, Kan^R and Cm^R)[36] was used as the target for the killing studies with our full system. All plasmids were prepared using the Gibson assembly method[37]. The sequences of CqsS, LuxU, LuxO, pQrr4, GFPmut3b, Art-085, Yebf-Art-085, promoters, RBS and terminators used in the study were taken from Genbank or the iGEM parts registry[38-39]. The backbone plasmids pBbE8k, pBbE6k, pBbA8c, pdCas9 were supplied by Addgene (Cambridge, Massachusetts, USA)[40]. All sequences (Supplementary Table 1) and plasmids (Supplementary Fig. 1) used in this study were prepared and analysed using the Benchling web-based sequence designer (Benchling, San Francisco, CA, USA). All protocols for transformations, PCR and DNA manipulation used in this work followed Sambrook or the manufacturer's manual and were optimized as needed[41]. Glycerol stocks of all cultures were made by mixing 500 µl of the overnight culture with 500 µl of 100% glycerol and stored in -80°C. For consistency, the overnight cultures for each experimental run were obtained by inoculating directly from their respective glycerol stocks.

Consumables and services

NEBuilder master mix for Gibson assembly was supplied by New England Biolabs (Ipswich, Massachusetts, USA). For PCR, we used the Q5 PCR kit supplied by New England Biolabs

(Ipswich, Massachusetts, USA). Purification kits (PCR, Gel, Miniprep) were supplied by Qiagen (Hilden, Germany). DNA concentrations were checked using a Nanodrop ND-1000 spectrophotometer. Commercial LB broth and agar supplied by BD (Franklin Lakes, New Jersey, USA) were used in all studies. LB was used as the medium for the characterization studies. Double concentrated LB (2xLB) was used to supplement spent cultures when needed. Kanamycin (50 μg/ml), ampicillin (100 μg/ml), gentamicin (10 μg/ml) or chloramphenicol (25 μg/ml) were added to the culture media for antibiotic selection when appropriate. All DNA sequencing services were supplied by 1st Base Company (Singapore). Primers and longer oligonucleotides were supplied by Integrated DNA Technologies (Coralville, Iowa, USA).

Microplate readings

All microplate readings were carried out using a Biotek Synergy HT microplate reader. The protocols for all readings with separately stated modifications are explained in each of the respective experimental sections. All cultures were grown in 96-well, transparent, flat-bottom microplates and distributed in triplicate with 300 or 200 (for killing assays) μl in each well. If an inducer was necessary, it was added to the well before the culture or directly into the tube with the culture at the appropriate concentration. Microplate readings were carried out with vigorous shaking for 6 h with OD_{600} and GFP fluorescence readings taken every 10 min. Relevant control and blank measurements were also taken in each microplate session.

Lysis-and-killing protein study

We constructed two different plasmids to characterize the expression of Art-085 and YebF-Art-085 in *E. coli*. Plasmid pBbE8k contained the pBAD promoter driving either the Art-085 or YebF-Art-085 gene, resulting in the pBbE8k-pBAD-rbsD-Art-085 (pArt085) and pBbE8k-pBAD-rbsD-YebF-Art-085 (pYArt085) plasmids, respectively. Each of the plasmids was transformed individually into *E. coli* TOP10 cells. Overnight cultures were diluted into 5 ml of fresh pre-warmed LB medium with the appropriate antibiotics for 2-3 h of exponential outgrowth at 37°C with shaking (225 rpm). Cultures were diluted to an initial OD_{600} of approximately 0.2 and aliquoted in triplicate with or without inducer (0.2% arabinose) in 96-well plates. The OD_{600} was measured for 6 h. Next, we placed the Art-085 gene under a constitutive promoter J23108 and the Lysis E7 gene under the pBAD promoter to verify whether Art-085 could efficiently kill *V. cholerae* (Vc-A1522-Tn7). Both genes were then incorporated into the pBbE8K vector. To incorporate gentamicin resistance inside our host, we cloned the aacC1 gene (NC_010410.1) under the constitutive promoter J23101 and placed it inside the pBbE8K vector. The result was the final test construct pKill1 (J23108-BBa_B0034-Art-085-BBa_B0015-pBAD-BBa_B0034-LysisE7-BBa_B0015-J23100-BBa_B0034-aacC1-BBa_B0015). As a control, we constructed a plasmid with Lysis E7 under the pBAD promoter and aacC1 under the J23101 promoter but lacking the Art-085 gene to generate pCtrl1 (pBAD-BBa_B0034-LysisE7-BBa_B0015-J23100-BBa_B0034-aacC1-BBa_B0015). Each of the plasmids was transformed individually into *E. coli* MG1655 wild-type cells. Briefly, both the strains were grown overnight, diluted 100 times in fresh LB supplemented with gentamicin and moved to a shaking incubator for 3 h of outgrowth to reach an OD_{600} of 0.7-1. The cultures were induced with 0.2% arabinose and allowed to grow for another 4 h to complete the lysis process. The supernatant was collected after centrifugation

and filtered using a 0.22 μm Millipore membrane filter unit. In parallel, pre-grown *V. cholerae* test strain cells were diluted to 0.5 OD_{600} using fresh LB media supplemented with gentamicin. To determine the dose-response curve of both the killer and control supernatants, we tested dilutions of 75%, 50%, 25%, 12% and 6% with fresh LB medium. The collected and diluted supernatants were then mixed with the prepared *V. cholerae* target cells at a 1:9 ratio (180 μl of the respective supernatants with 20 μl of *V. cholerae* culture) and aliquoted into 96-well plates. Subsequently, the cultures were moved to the microplate and tested in the reader for another 6 h.

Lysis circuit study

The pColE1 ori-containing plasmid from our previous work[18] was modified by exchanging the anti-BBa_J23115 gRNA with anti-pBAD gRNA. Additionally, its kanamycin resistance gene was exchanged for ampicillin resistance to match the target *V. cholerae* strain. The anti-pBAD gRNA was designed using the Benchling genome engineering tool (Benchling, CA, USA). It uses a model derived by Doench et al. for on-target CRISPR cutting efficiency and a second model created by Hsu et al. for off-target CRISPR cutting efficiency to present the user with two scores (from 1 to 100 points) for each of the gRNAs, one for on-target cutting efficiency and a second for off-target cutting efficiency. In both cases, the maximum score of 100 points is desired[42-43]. Additionally, we performed a BLAST run for each of the gRNAs against the MG1655 *E. coli* genome to determine whether there were any potential binding sites. Binding sites were identified based on several criteria, which all had to be achieved for any given gRNA for it to be considered a possible off-target binding site. The criteria were as follows. First, there could not be any mismatches between the gRNA and target sequence in the first seven bp (seed region). In addition, the homologous region could not be shorter than 12 bp. This approach resulted in our redesigned new sensor plasmid pSENSE (pLlac-O1-BBa_B0034-LuxO-BBa_B0015-p66-BBa_B0034-CqsS-BBa_B0015-p66-BBa_B0034-LuxU-BBa_B0015-tpQrr4-antipBADgRNA-BBa_B0015).

Next, the p15A ori-containing plasmid had the constitutive BBa_J23105 promoter replaced with the arabinose-inducible (pBAD) promoter and the accompanying AraC gene for its regulation. Subsequently, the GFP gene was replaced with the YebF-Art-085 gene encoding the lysis protein. Thus, the lysis-inducing plasmid pKill2 (GabDP2-BBa_B0034_dCas9-BBa_B0015_pBAD_rbsD_YebF-Art-085-BBa_B0015) was created. Next, the lysis-inducing plasmid from the previous study was expanded by incorporating the Art-085 gene with a strong promoter (p66) and a strong RBS, resulting in our final killing plasmid pKill3 (GabDP2-BBa_B0034_dCas9-BBa_B0015_pBAD_rbsD_YebF-Art-085-BBa_B0015-p66-BBa_B0034_Art-085_BBa_B0015). These new lysis (pKill2) and killing (pKill3) plasmids were co-transformed with the new sensor plasmid (pSENSE).

The characterization assay for *E. coli* cells harbouring either the lysis-inducing system (pSENSE + pKill2) or the final killing system (pSENSE + pKill3) was carried as follows. Overnight cultures of *V. cholerae* and *E. coli* were sub-cultured by diluting 100 times and transferred to a shaking incubator for 4 h of outgrowth. Next, the supernatant from the cultures was obtained by centrifugation and filter sterilization using 0.22 μm Millipore membrane filters. Subsequently, overnight cultures of the tested constructs were diluted 100 or 25 (for high starting OD_{600} tests)

times in their respective supernatants. Such cultures were first moved to a shaking incubator for 2 h of outgrowth and then supplemented with inducers and moved to microplate and tested in the reader for another 6 h. Following earlier reports[44-45], cell lysis was defined as a visible negative change of OD_{600} in time compared to the control culture. In line with this, cultures that are not growing i.e. showing no visible change of OD_{600} in time are considered not lysing.

Killing study

The killing assays were carried out as follows. Overnight cultures of *V. cholerae* and *E. coli* were re-cultured by diluting 100 times in fresh LB and were transferred to a shaking incubator for 4 h of outgrowth. Next, the supernatants from the respective cultures were collected by centrifugation and filter sterilized with 0.22 μm Millipore membrane filters. The overnight cultures of our engineered *E. coli* carrying either the lysis-inducing system or final killing system were diluted 25 times in their respective supernatants with the appropriate antibiotics (ampicillin and chloramphenicol). The cultures were first moved to a shaking incubator for 2 h of outgrowth and then supplemented with inducers and maintained in the shaking incubator for another 3 h to complete the lysis process. After 3 h, the supernatants from their respective cultures were collected by centrifugation followed by filtration with 0.22 μm Millipore membrane filters. In parallel, overnight cultures of *V. cholerae* target cells were diluted to an OD_{600} of 0.5 with fresh 2xLB. The collected supernatants were then mixed with the prepared *V. cholerae* (Vc-*hapR*-RFP) target cells at a 1:9 ratio (180 μl of respective supernatants with 20 μl of *V. cholerae* culture) and aliquoted into 96-well plates. Subsequently, the cultures were moved to microplate and incubated in the reader for another 6 h.

The time-kill assay was performed by preparing serial dilutions of *V. cholerae* cultures exposed to the supernatants of our engineered *E. coli* carrying the final system grown in *E. coli* (control) or *V. cholerae* (activating) supernatant induced with 0.001% arabinose that were run in tubes in a shaking incubator in parallel with the microplate assay. The dilutions were made from the inoculum, 0, 30, 60, 90, 120, 180, 240, 300 and 360 min time points and with dilution ratios ranging from 10^2 to 10^9 times. This approach set the lower detection limit to 100 CFU and the higher detection limit to 10^9 CFU. The dilutions were plated onto LB plates without antibiotics and incubated overnight at 37°C for 14 h, after which colony counts were performed.

The agar overlay assay was performed by preparing an LB agar plate and dividing the plate into four equal quadrants, with each quadrant receiving three 20 μl droplets of supernatant (either from *E. coli* or *V. cholerae* supernatant-induced cultures of our engineered *E. coli*), with the final system having 0.001% arabinose added. After the droplets had dried, overnight cultures of *V. cholerae* target cells were homogeneously mixed with a soft LB agar solution (10 g/l tryptone, 5 g/l yeast extract, 10 g/l sodium chloride and 7 g/l agar) and gently poured onto the agar plates. The agar plates with the soft agar overlaid were maintained in the incubator at 37°C, and photographs were taken under a white light source after 4 h of incubation.

Author information

Corresponding Author

* Chueh Loo Poh – poh.chuehloo@nus.edu.sg

Author Contributions

CLP, MBH and PJ conceived the idea of the system. PJ and MBH have performed the design, construction and testing of the circuits. JWY has constructed the model used in the study. CLP and SL have advised MBH, PJ and JWY on their respective parts. The manuscript was written through contributions of all authors.

Acknowledgement

We would like to thank the financial support from Ministry of Education, Singapore. This work was funded under MoE Tier 2 grant (AcRF ARC43/13). Holowko M. B. would like to thank Agency for Science, Technology and Research (A*STAR) of Singapore for providing him with funding un-der Singapore International Graduate Award (SINGA). We would also like to thank A/Prof Diane McDougald from SCELSE, Singapore for helping us with obtaining the *Vibrio cholerae* strains used in this study. We would like to thank Batika Saxena from www.batikasaxena.com for preparing the illustrations used in the article.

Supporting Information

1. Supplementary Figure 1: List of plasmids used in this study.
2. Supplementary Figure 2: Growth curves of *V. cholerae A1552* in (a) pKill1 and (b) pCtrl1 supernatant dilutions.
3. Supplementary Table 1: List of sequences of all the genes and genetic parts used in this study.
4. Model development.
    a. Supplementary Figure 3: Parameters estimation of constitutive transcription determined by three promoters (p66, p51, p108) after fitting the models (shown in lines) to the measured characterization data (shown in symbols).
    b. Supplementary Figure 4: Parameters estimation of translation determined by three different RBSs (rbs32, rbs34, rbs64) after fitting the models (shown in lines) to the measured characterization data (shown in symbols).
    c. Supplementary Figure 5: Model simulations for the constitutive transcription and translation of killing protein Art-085. **(a)** Simulated concentration for the level of mRNA concentration after reaching steady state. **(b)** Simulated concentration for the Art-085 proteins after steady-state level.
    d. Supplementary Table 2: Mathematical formulation to model the eradicate system under both *E.coli* (control) and *V. cholerae* supernatants.
    e. Supplementary Table 3: List of parameters used in our model.
    f. Supplementary Table 4: List of initial conditions for the variables used in our model.

References

1. Braff, D.; Shis, D.; Collins, J. J., Synthetic biology platform technologies for antimicrobial applications. *Advanced Drug Delivery Reviews* **2016,** *105, Part A*, 35-43.
2. Ruder, W. C.; Lu, T.; Collins, J. J., Synthetic Biology Moving into the Clinic. *Science* **2011,** *333* (6047), 1248.

3. Who, Weekly epidemiological record. **2014,** *31*, 345-356.
4. Meehan, C. D. M., Howard, Cholera, Historical. *The Encyclopedia of Microbiology* **2000,** *I*.
5. Harris, J. B.; LaRocque, R. C.; Qadri, F.; Ryan, E. T.; Calderwood, S. B., Cholera. **2012,** *379*, 2466-2476.
6. Pastor, M.; Pedraz, J. L.; Esquisabel, A., The state-of-the-art of approved and under-development cholera vaccines. *Vaccine* **2013**.
7. Sneha, K. G.; Anas, A.; Jayalakshmy, K. V.; Jasmin, C.; Das, P. V. V.; Pai, S. S.; Pappu, S.; Nair, M.; Muraleedharan, K. R.; Sudheesh, K.; Nair, S., Distribution of multiple antibiotic resistant Vibrio spp across Palk Bay. *Regional Studies in Marine Science* **2016,** *3*, 242-250.
8. Hammer, B. K.; Bassler, B. L., Quorum sensing controls biofilm formation in Vibrio cholerae. *Molecular microbiology* **2003,** *50* (1), 101-104.
9. Jung, S. A.; Chapman, C. A.; Ng, W. L., Quadruple quorum-sensing inputs control Vibrio cholerae virulence and maintain system robustness. *PLoS pathogens* **2015,** *11* (4), e1004837.
10. Krukonis, E. S.; DiRita, V. J., From motility to virulence: Sensing and responding to environmental signals in Vibrio cholerae. *Current opinion in microbiology* **2003,** *6* (2), 186-190.
11. Miller, M. B.; Skorupski, K.; Lenz, D. H.; Taylor, R. K.; Bassler, B. L., Parallel quorum sensing systems converge to regulate virulence in Vibrio cholerae. *Cell* **2002,** *110* (3), 303-314.
12. Boyaci, H.; Shah, T.; Hurley, A.; Kokona, B.; Li, Z.; Ventocilla, C.; Jeffrey, P. D.; Semmelhack, M. F.; Fairman, R.; Bassler, B. L.; Hughson, F. M., Structure, Regulation, and Inhibition of the Quorum-Sensing Signal Integrator LuxO. *PLoS Biol* **2016,** *14* (5), e1002464.
13. Ng, W. L.; Perez, L. J.; Wei, Y.; Kraml, C.; Semmelhack, M. F.; Bassler, B. L., Signal production and detection specificity in Vibrio CqsA/CqsS quorum-sensing systems. *Molecular microbiology* **2011,** *79* (6), 1407-17.
14. Neiditch, M. B.; Federle, M. J.; Miller, S. T.; Bassler, B. L.; Hughson, F. M., Regulation of LuxPQ receptor activity by the quorum-sensing signal autoinducer-2. *Molecular cell* **2005,** *18* (5), 507-518.
15. Jobling, M. G.; Holmes, R. K., Characterization of hapR, a positive regulator of the Vibrio cholerae HA/protease gene hap, and its identification as a functional homologue of the Vibrio harveyi luxR gene. *Molecular microbiology* **1997,** *26* (5), 1023-1034.
16. Saeidi, N.; Wong, C. K.; Lo, T.-M.; Nguyen, H. X.; Ling, H.; Leong, S. S. J.; Poh, C. L.; Chang, M. W., Engineering microbes to sense and eradicate Pseudomonas aeruginosa, a human pathogen. *Molecular Systems Biology* **2011,** *7*, 521-521.
17. Gupta, S.; Bram, E. E.; Weiss, R., Genetically Programmable Pathogen Sense and Destroy. *ACS Synthetic Biology* **2013,** *2* (12), 715-723.
18. Holowko, M. B.; Wang, H.; Jayaraman, P.; Poh, C. L., Biosensing Vibrio cholerae with Genetically Engineered Escherichia coli. *ACS Synthetic Biology* **2016**.
19. Kelly, R. C.; Bolitho, M. E.; Higgins, D. A.; Lu, W.; Ng, W.-L.; Jeffrey, P. D.; Rabinowitz, J. D.; Semmelhack, M. F.; Hughson, F. M.; Bassler, B. L., The Vibrio cholerae quorum-sensing autoinducer CAI-1: analysis of the biosynthetic enzyme CqsA. *Nat Chem Biol* **2009,** *5* (12), 891-895.
20. Larson, M. H.; Gilbert, L. A.; Wang, X.; Lim, W. A.; Weissman, J. S.; Qi, L. S., CRISPR interference (CRISPRi) for sequence-specific control of gene expression. *Nat Protoc* **2013,** *8* (11), 2180-2196.

21. Qi, L. S.; Larson, M. H.; Gilbert, L. A.; Doudna, J. A.; Weissman, J. S.; Arkin, A. P.; Lim, W. A., Repurposing CRISPR as an RNA-guided platform for sequence-specific control of gene expression. *Cell* **2013,** *152* (5), 1173-1183.
22. Schmelcher, M.; Donovan, D. M.; Loessner, M. J., Bacteriophage endolysins as novel antimicrobials. *Future microbiology* **2012,** *7* (10), 1147-1171.
23. Gerstmans, H.; Rodríguez-Rubio, L.; Lavigne, R.; Briers, Y., From endolysins to Artilysin®s: novel enzyme-based approaches to kill drug-resistant bacteria. *Biochemical Society transactions* **2016,** *44* (1), 123-128.
24. Skerlavaj, B.; Benincasa, M.; Risso, A.; Zanetti, M.; Gennaro, R., SMAP-29: a potent antibacterial and antifungal peptide from sheep leukocytes. *FEBS letters* **1999,** *463* (1-2), 58-62.
25. Briers, Y.; Walmagh, M.; Grymonprez, B.; Biebl, M.; Pirnay, J.-P.; Defraine, V.; Michiels, J.; Cenens, W.; Aertsen, A.; Miller, S.; Lavigne, R., Art-175 Is a Highly Efficient Antibacterial against Multidrug-Resistant Strains and Persisters of Pseudomonas aeruginosa. *Antimicrobial agents and chemotherapy* **2014,** *58* (7), 3774-3784.
26. Defraine, V.; Schuermans, J.; Grymonprez, B.; Govers, S. K.; Aertsen, A.; Fauvart, M.; Michiels, J.; Lavigne, R.; Briers, Y., Efficacy of Artilysin Art-175 against Resistant and Persistent Acinetobacter baumannii. *Antimicrobial agents and chemotherapy* **2016,** *60* (6), 3480-3488.
27. Zhang, G.; Brokx, S.; Weiner, J. H., Extracellular accumulation of recombinant proteins fused to the carrier protein YebF in Escherichia coli. *Nat Biotech* **2006,** *24* (1), 100-104.
28. Holowko, M. B.; Wang, H.; Jayaraman, P.; Poh, C. L., Biosensing Vibrio cholerae with Genetically Engineered Escherichia coli. *ACS Synthetic Biology* **2016,** *5* (11), 1275-1283.
29. Ausubel, F. M., *Short protocols in molecular biology : a compendium of methods from current protocols in molecular biology Vol. 1. Vol. 1*. Wiley: [S.l.], 2002.
30. Brophy, J. A. N.; Voigt, C. A., Principles of genetic circuit design. *Nat Meth* **2014,** *11* (5), 508-520.
31. Briers, Y.; Walmagh, M.; Van Puyenbroeck, V.; Cornelissen, A.; Cenens, W.; Aertsen, A.; Oliveira, H.; Azeredo, J.; Verween, G.; Pirnay, J.-P.; Miller, S.; Volckaert, G.; Lavigne, R., Engineered Endolysin-Based "Artilysins" To Combat Multidrug-Resistant Gram-Negative Pathogens. *mBio* **2014,** *5* (4).
32. Focareta, A.; Paton, J. C.; Morona, R.; Cook, J.; Paton, A. W., A recombinant probiotic for treatment and prevention of cholera. *Gastroenterology* **2006,** *130* (6), 1688-1695.
33. Duan, F.; March, J. C., Engineered bacterial communication prevents Vibrio cholerae virulence in an infant mouse model. *Proceedings of the National Academy of Sciences* **2010,** *107* (25), 11260-11264.
34. Kothary, M. H.; Babu, U. S., INFECTIVE DOSE OF FOODBORNE PATHOGENS IN VOLUNTEERS: A REVIEW. *Journal of Food Safety* **2001,** *21* (1), 49-68.
35. Lim, B.; Beyhan, S.; Meir, J.; Yildiz, F. H., Cyclic-diGMP signal transduction systems in Vibrio cholerae: modulation of rugosity and biofilm formation. *Mol Microbiol* **2006,** *60* (2), 331-348.
36. Sun, S.; Kjelleberg, S.; McDougald, D., Relative Contributions of Vibrio Polysaccharide and Quorum Sensing to the Resistance of Vibrio cholerae to Predation by Heterotrophic Protists. *PLOS ONE* **2013,** *8* (2), e56338.
37. Gibson, D. G.; Young, L.; Chuang, R.-Y.; Venter, J. C.; Hutchison, C. A.; Smith, H. O., Enzymatic assembly of DNA molecules up to several hundred kilobases. *Nature methods* **2009,** *6* (5), 343-345.

38. Hase, C. C.; Finkelstein, R. A., Cloning and nucleotide sequence of the Vibrio cholerae hemagglutinin/protease (HA/protease) gene and construction of an HA/protease-negative strain. *J Bacteriol* **1991,** *173* (11), 3311-7.
39. Promoters/Catalog/Anderson - parts.igem.org.
40. Lee, T. S.; Krupa, R. A.; Zhang, F.; Hajimorad, M.; Holtz, W. J.; Prasad, N.; Lee, S. K.; Keasling, J. D., BglBrick vectors and datasheets: A synthetic biology platform for gene expression. *Journal of biological engineering* **2011,** *5*, 12.
41. Sambrook, J., *Molecular cloning : a laboratory manual / Joseph Sambrook, David W. Russell*. Cold Spring Harbor Laboratory: Cold Spring Harbor, N.Y, 2001.
42. Hsu, P. D.; Scott, D. A.; Weinstein, J. A.; Ran, F. A.; Konermann, S.; Agarwala, V.; Li, Y.; Fine, E. J.; Wu, X.; Shalem, O.; Cradick, T. J.; Marraffini, L. A.; Bao, G.; Zhang, F., DNA targeting specificity of RNA-guided Cas9 nucleases. *Nat Biotechnol* **2013,** *31* (9), 827-832.
43. Doench, J. G.; Hartenian, E.; Graham, D. B.; Tothova, Z.; Hegde, M.; Smith, I.; Sullender, M.; Ebert, B. L.; Xavier, R. J.; Root, D. E., Rational design of highly active sgRNAs for CRISPR-Cas9-mediated gene inactivation. *Nat Biotechnol* **2014,** *32* (12), 1262-1267.
44. Repaske, R., Lysis of gram-negative organisms and the role of versene. *Biochimica et biophysica acta* **1958,** *30* (2), 225-232.
45. Pasotti, L.; Zucca, S.; Lupotto, M.; Cusella De Angelis, M. G.; Magni, P., Characterization of a synthetic bacterial self-destruction device for programmed cell death and for recombinant proteins release. *Journal of Biological Engineering* **2011,** *5*, 8-8.

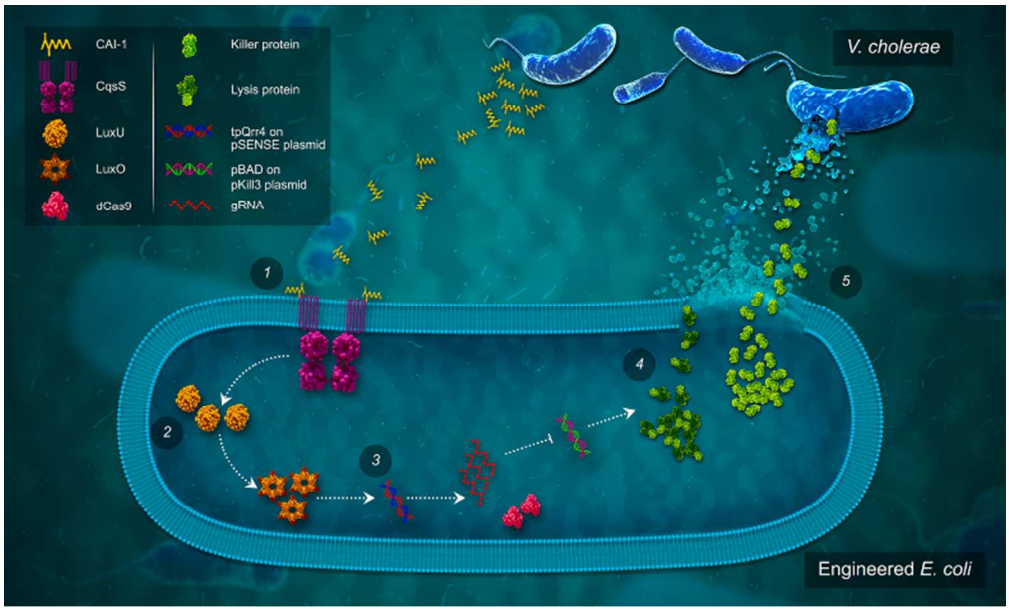

66x39mm (300 x 300 DPI)